

7184-~~MA~~-01)ENV

DTIC.

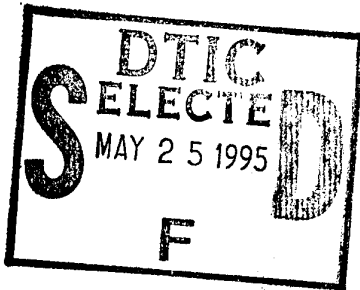
ATOMS IN STRONG FIELDS

Final Technical Report

by

Giulio Casati: Principal Investigator

April 1995



United States Army

EUROPEAN RESEARCH OFFICE OF THE U.S. ARMY

London, England

CONTRACT NUMBER N68171-94-M-5310

Centro di Cultura Scientifica "A. Volta"

Villa Olmo - 22100 Como - Italy

Approved for Public Release: distribution unlimited

19950524 029

DTIC QUALITY INSPECTED 5

Contents

1	Background	3
2	Theoretical Approach	4
2.1	Qualitative Description	4
2.2	Statement of Problems.	7
2.3	The Kicked Hydrogen Atom	8
2.4	Results	10
3	An aside on the autoionization of Molecules.	12
3.1	Background	12
3.2	Theory.	13
3.3	Results.	15
4	Conclusions and recommendations.	16
5	Figure Captions.	17
6	Bibliography.	18

Accession For	
NTIS CRA&I	<input checked="" type="checkbox"/>
DTIC TAB	<input type="checkbox"/>
Unannounced	<input type="checkbox"/>
Justification	
By	
Distribution /	
Availability Codes	
Dist	Avail and/or Special
A-1	

1 Background

The response of a bound electron to an external monochromatic field is a complicated process, that gives rise to a variety of phenomena. This problem has proven much richer than could be suspected at the origins of quantum mechanics. This is hardly surprising, because at the root of its richness lies the full complicity of classical nonlinear dynamics, that only in recent times we have begun to explore.

In 1974 Bayfield and Koch found that the ionization of highly excited hydrogen atoms by microwave fields has a threshold character with respect to field strength: it is very small at very small intensity but it increases abruptly at a certain threshold intensity. This was found to be an essentially classical phenomenon, the observed threshold being practically the same as the classical threshold above which the classical dynamics of the electron becomes chaotic. 'Chaotic' ionization was extensively investigated in the 80's, both experimentally and theoretically. The important result was thus established, that classical chaotic effects have a counterpart in quantum mechanics, associated with phenomena in the atomic domain that lie beyond the grasp of conventional purely quantal theoretical methods.

This very idea lies at the core of the research summarized in this report, which was aimed at a classical analysis of the 'intense field stabilization' (IFS) effect. This effect is expected to appear on increasing the field strength still further[1].

When a beam of hydrogen atoms passes through a linearly polarized radiation field of given frequency and intensity, a fraction of the total number of atoms will be ionized as a consequence of the perturbation produced by the field on the motion of the atomic electrons. This fraction, which defines the *probability of ionization*, will be more or less large, depending on the actual values of the frequency ν , of the intensity I , and of the time of interaction. According to common intuition, if the radiation frequency and the interaction time are fixed, stronger fields should be expected to produce a stronger ionization - in other words, the ionization probability should be a monotonic function of the field intensity at fixed frequency.

A number of theoretical studies suggest that this may not be the case.

According to these studies, the ionization probability will at first increase with the field intensity as expected, but when the intensity becomes large enough it will start to decrease, i.e. the atom will become increasingly stable against field-induced ionization. This surprising effect is called stabilization. It was first predicted on purely quantum grounds by Pont and Gavrila in 1990, and has since become a topic of lively interest. It is not yet clear whether the effect can be detected in laboratory experiments, because the existing theories do not yield precise estimates for the range of parameter values where the effect should be observable. The analysis by Gavrila&Pont has been followed by numerical simulations of the quantum dynamics by Su, Eberly and Javanainen 1991 and by Kulander, Schafer and Krause 1991. These studies have exposed stabilization for small initial quantum numbers $1 \div 6$ at field intensity $\sim 1 a.u.$ and frequency on the order of the binding energy of the atom. Such conditions would make stabilization even more puzzling, binding it to occur in a situation in which absorption of even one single photon leads to ionization; moreover, they would place the observation of the effect beyond the reach of current laser technology.

More recent studies have indicated that stabilization would occur also at significantly lower frequencies, provided that the initial state of the atom has a nonzero magnetic quantum number along the direction of the field. It has been remarked by Gavrila et al. 1992 that the frequency may be greatly reduced if one allows for high initial magnetic quantum number, to the extent that the effect should be observable in laboratory experiments at current laser performances.

2 Theoretical Approach

2.1 Qualitative Description

Our own approach to the stabilization problem is based on the idea that IFS is basically a classical phenomenon and that some of its quantitative features can be caught by an analysis based on classical mechanics. In the light of the above reviewed findings about chaotic ionization, we maintain that classical nonlinear effects do have a relevance in the photoionization problem and that classical estimates can be quite effective. As a matter of fact, Grobe et al

1991, Grochmalicki et al 1991, Bowden et al 1991 have investigated classical versions of a simplified model by Su et al.. (a one-dimensional model with a 'smoothed' Coulomb potential) and have concluded that most features of stabilization already occur in a classical context.

We use a simple Keplerian model, in which the electron moves under the combined effect of the Coulomb field and of the radiation field. The Hamiltonian of this model is

$$H = \frac{p^2}{2} - \frac{1}{r} + z\epsilon \sin(\omega t) \quad (1)$$

where r is distance from the nucleus and the coordinate z is measured along the direction of the (linearly polarized) external field. In eqn.(1) atomic units were used, in which various constants have a unit value; ϵ and ω are the field intensity and frequency. The Hamiltonian (1) describes a highly nonlinear dynamics. Since the direction of the external force field is fixed in time, there is one conserved quantity, namely the projection m of the electron angular momentum l along the field direction; this we call the magnetic number.

Our analysis starts with a simple qualitative argument. If the electron were subjected *only* to the external field then its motion could be simply described as an rectilinear uniform motion at constant velocity v with a superimposed oscillation of amplitude ϵ/ω^2 . The work done by the field in one field period would then be

$$W = -\epsilon \int_0^{2\pi\omega^{-1}} v \sin(\omega t) dt = 0 \quad (2)$$

On the other hand, the Coulomb force would enforce a change in time of the drift velocity v . Although eqn (2) would be still approximately valid when the electron is far from the nucleus, near the nucleus the change of v during one period would be large, leading to a significant energy transfer. In this way we see that the external field is most effective in perturbing the electron dynamics when the electron is close to the nucleus, so that the main contribution to ionization comes from close encounters with the nucleus. Now suppose that prior to the switching on of the field the electron was moving along a Keplerian ellipse with given angular momentum l and magnetic number m . Roughly speaking, the field will superimpose on this motion an oscillation of width $\epsilon\omega^{-2}$ along the field direction. The global effect of this oscillation will be qualitatively different according to whether

$m = 0$ or $m \neq 0$. In the former case the direction of the field lies in the plane of the orbit, and the field induced oscillation along that direction will bring sooner or later the electron close to the nucleus; during each such encounter it will absorb much energy from the field and will be consequently ionized in a relatively short time. Instead, if $m \neq 0$, the large field oscillation will carry the electron away from the plane of the orbit and will therefore keep it a long time far from the nucleus, where its average energy won't change very much. In essence, this is the mechanism of classical stabilization.

This rough intuitive picture, which decouples the motion in an orbital part plus a field oscillation, clearly rests on the assumption that the change of the orbital 'drift' velocity during one period due to the Coulomb force is small. This condition is the better satisfied, the larger the field frequency. In a sense, stabilization occurs when the Coulomb force acts as an adiabatic perturbation of the free field motion. This adiabaticity is violated either at small frequencies or at small values of m , that allow for frequent encounters with the nucleus. In this way we have obtained a qualitative understanding of the role of the parameters m and ω . Let us now briefly sketch some more details.

A more precise analysis starts with a well-known coordinate transformation (Kramers-Henneberger transformation). Instead of studying the dynamics in the fixed 'laboratory' reference frame we move to a moving reference frame which oscillates along the direction of the field with the frequency of the field itself. In this new frame the nucleus is not at rest but is itself oscillating with the frequency ω , and the electron is only subject to the potential of this moving charge. If the amplitude and frequency of the oscillations are large enough, then a convenient approximation for the moving-charge potential is obtained by time-averaging.

By using the time-averaged potential in place of the exact, time-dependent one we get an effective time-independent Hamiltonian. The averaged Hamiltonian is conveniently written in cylindrical coordinates ρ, z, ϕ with the z axis along the direction of the field, and is that of an electron moving in the field of a charge distributed along a 'thread' of length ϵ/ω^2 (with a certain time-independent density). This field has still a singularity at $\rho = 0$, which is however of logarithmic type, hence of a much milder sort than the original Coulomb singularity. On the other hand the centrifugal term (3d term in eqno(2)) has a much stronger singularity and thus it prevents the electron from coming appreciably close to the thread, *as long as the averaged*

Hamiltonian can be assumed to be a constant.

In other words, the combination of the potential of the thread and of the centrifugal potential produces a potential well inside which the electron can be trapped. In our theory of ref.([2]) this very trapping is responsible for stabilization. A quantitative condition for that is gotten from the requirement of adiabatic invariance of the averaged Hamiltonian . The condition reads

$$\epsilon > \epsilon_{stab} = \alpha \frac{\omega}{m} \quad (3)$$

where α is a numerical constant.

The existence of the stabilization effect in the classical model (1) and the dependence of the stabilization threshold on frequency and magnetic number predicted by (3) have been confirmed by numerical simulations of the classical dynamics.

2.2 Statement of Problems.

To summarize the previous discussion:

the stabilization of hydrogen atoms in strong monochromatic fields is strongly suggested by quantum numerical simulations and by quantum theoretical arguments that do not however provide precise estimates for the experimental conditions under which the effect should be observed. On the other hand there is sound numerical evidence that the effect is already present in classical mechanics; moreover, we have a rough quantitative predictions for the classical effect. Remarkably, this estimate predicts stabilization of Rydberg atoms ($n \sim 70$) at reasonable field intensities $\epsilon \sim 2 \times 10^3 V/cm$ with frequencies in the microwave region.

Nevertheless, this (largely heuristic) classical analysis is still wanting, and its indication about the actual observability of IFS calls for a more refined investigation, that may account for important aspects . In particular, a very important , as yet poorly understood, problem is

- what is the role of chaos in the classical ionization process ? classical ionization at low field is well known to be due to the onset of chaos. What is the nature of the motion in the stabilized regime?

Classical analysis, both numerical and theoretical, is technically difficult. In addition, it is encumbered by several accessory features whose relevance to the IFS is not clear. For example, the effective Hamiltonian hinted to above is fairly complicated itself and exhibits a remarkable feature named 'dichotomy': in the reference frame oscillating with the external field, the nucleus itself oscillates and produces an average Coulomb field quite similar to the field due to a charge continuously distributed along its trajectory. Since the nucleus spends a large part of its time in the vicinity of the turning points of its trajectory, this charge distribution is highly non homogeneous and looks like a sort of dumb-bell. At low field the combination of "dumb-bell" and centrifugal potentials produces an effective potential well which has a single minimum; however, as the field increases the potential well is more and more strained and above a certain field intensity it splits into a double-well potential which has two minima located close to the extrema of the dumb-bell. This metamorphosis of the average potential experienced by the electron in the moving frame has been often considered as a key ingredient of IFS, both in the quantum [5] and in the classical description[3].

In order to get rid of accessory features and to make numerical analysis easier we have used a simpler model that nevertheless retains all the essential ingredients of IFS. In this model the external perturbing field is not monochromatic but consists of a train of δ -like pulses, or kicks, of alternate sign. This kicked model offers the following advantages:

- it is very convenient for numerical simulation; an exhaustive map of the dependence of the ionization probability on the various parameters can be obtained;
- it still exhibits IFS;
- it *does not* exhibit dichotomy, so that the latter turns out to be inessential
- ;
- from the viewpoint of the above sketched quantitative theory of ours it is expected to behave exactly as the realistic monochromatic model.

2.3 The Kicked Hydrogen Atom

The technical tool we have used is a modified model in which a classical 3 dimensional hydrogen atom is subjected to a periodic sequence of δ -like pulses of fixed strength and direction and alternating sign. The advantage of this model is that its numerical simulation is very economic as compared to

that of the more realistic, monochromatically driven atom. Its Hamiltonian reads

$$H(\vec{p}, \vec{r}, t) = \frac{p^2}{2} - \frac{1}{r} + \frac{2\epsilon z}{\omega} \sum_{n=-\infty}^{+\infty} (-1)^n \delta(t - \frac{nT}{2}) \quad (4)$$

where $\vec{r} = (x, y, z)$, $T = 2\pi/\omega$, and atomic units were used. The dipole approximation is used, and the field is polarized in the z -direction.

The evolution defined by (4) over one period $T = \frac{2\pi}{\omega}$ is given by a product of four maps. The first of these describes a free Keplerian motion over a time $\frac{T}{2}$; the second, a "kick" which discontinuously changes p_z into $p_z + \frac{2\epsilon}{\omega}$; next comes one more free Kepler motion, followed by one more kick changing p_z by $-\frac{2\epsilon}{\omega}$. Iteration of this four-factor map yields a stroboscopic evolution defined by (4) which can be computed with considerably less numerical effort than that required for the simulation of (1) over a comparable number of periods.

A "Kramers-Henneberger transformation" can be performed to a reference frame which oscillates in the z -direction according to a sawtooth. The moving nucleus produces an uniform average charge distribution. The combination of the corresponding average potential and of the centrifugal potential yields the effective potential, that, unlike the case of a monochromatic driving, has always a single minimum.

The dependence of the ionization probability on the field parameters ϵ and ω is illustrated by the "phase diagram" of Fig.1, which displays the survival probability after a fixed physical time for different values of ϵ and ω . It was constructed in the following way[CGM]. First we have chosen 60 evenly spaced points on the horizontal axis and 80 evenly spaced points on the vertical axis. Having thus discretized the region shown in Fig.1 by means of 4800 points, for each of these we have numerically computed 100 orbits having initial action variables $n = 1, l = 0.3, m = 0.25$ and randomly distributed angle variables. Due to well-known scaling properties, cases with initial $n \neq 1$ can be reduced to cases $n = 1$ by using scaled variables $\omega n^3, \epsilon n^4, l/n, m/n$.

The survival probability was determined as the fraction of orbits that remained within a distance $r = 500$ from the nucleus after a time corresponding to approximately 500 kepler periods at $n = 1$. Kicks were smoothly switched on, i.e. ϵ was linearly increased from zero to its nominal value during a finite number of kicks (10 kicks for the case of Fig.1). The main qualitative feature of Fig.1 is represented by two wedge-shaped regions of high survival proba-

bility. These regions are separated by a "death valley" that becomes deeper when moving to higher frequencies. The lower stable region is located at small ϵ and corresponds to a regime of dynamically stable motion; the upper region is the one corresponding to IFS.

2.4 Results

A first basic question is about the dependence of the stabilization probability on the interaction time. During a longer interaction time, some of the surviving orbits contributing in the grey regions of fig.1 would be ionized, so that the figure would overall turn to paler tones of grey. What changes would occur in the geography of fig.1 if the figure were reproduced with a longer interaction time? In particular, does the functional form of the stabilization threshold depend on time? This is of course a crucial question for the practical usefulness of our theoretical estimates.

To answer this question, we have chosen three points in the (ϵ, ω) plane of Fig.1, respectively located (a) deep in the lower stable region, (b) still in that region, but not far from its upper border, (c) in the IFS region. For each of these we have computed the survival probability P_s as a function of the interaction time, over an interval from 100 to 35000 pulses. Results are shown in fig.(2). They indicate that the upper border of the lower region is not stable in time and must be expected to move downwards on increasing the interaction time; instead, the IFS region appears to be essentially stable on a very long time scale.

Next one would like to understand the dynamical origin of the various stability regions.

An obvious reference problem for understanding the nature of the lower stable region is the low-field stability of monochromatically driven atoms, which has been extensively studied. The excitation process is known to be determined by a typical KAM scenario, with distorted KAM tori gradually disappearing on increasing ϵ . In the KAM region, the only possible ionization mechanism is Arnol'd diffusion of unstable orbits between surviving tori; this is a very slow process, that would produce a substantial stability over not too long time scales. We ignore whether KAM tori survive at low field in our case, too.

In any case, the border of the lower stable region is determined by a chaotic ionization mechanism very similar to the one widely discussed for

the case of monochromatic driving. Far from the nucleus the electron is moving on an almost perfect Keplerian ellipse in spite of the periodic kicks. In fact subsequent kicks have opposite sign and compensate each other almost exactly, except when the electron comes close to the nucleus: there its velocity changes significantly between subsequent kicks and the external field is therefore most effective. From close encounters with the nucleus the electron emerges on a different almost unperturbed ellipse and the process is repeated a number of times, until a particularly energetic encounter with the nucleus sets the electron on an escape route. In the chaotic regime, the sequence of jumps can be pictured as a random walk (in energy) eventually leading to ionization. The corresponding diffusion coefficient, however, decreases on increasing the external frequency, and this explains why, at fixed interaction time, the survival probability is found to be an increasing function of ω .

To get a more refined test, we have numerically computed Maximal Lyapunov Exponents (MLE) at various values of the field and for a fixed frequency, (fig.3). This was done by numerically computing the rate of exponential separation of orbits initially close to each other, not in real time but in a fictitious time proportional to the number of passages at the aphelion. This was necessary because excitation, hence ionization, only occurs close to the aphelion. The higher the electron is excited in the principal action n , the longer it stays away from the nucleus, moving on an almost perfect unperturbed ellipse. Thus, even in the case when the sequence of passages at the aphelion affects the motion of the electron in a chaotic way, the appearance of longer and longer quasi-regular strings in the motion of the electron far from the aphelion would force Lyapunov exponents in real time to vanish.

In fig.3 we show the MLE as a function of the field intensity at fixed frequency. The MLE is significantly different from zero even below the stability border resulting from Fig.1, which implies that this border is not stable in time, because a large fraction of the surviving orbits are in fact chaotic and would ionize in a longer time. The actual stability border, where the MLE falls to the level of numerical errors, is significantly lower.

We have computed MLE's in the IFS region, too, for stabilized (non-ionizing) trajectories. Such orbits have the typical appearance shown in Figs.4,5. In particular, Fig.5 shows that stabilized orbits look like the trajectories of an electron moving in the average KH potential. Numerically computed MLE for such orbits fall within the range of numerical noise, im-

plying that the stabilized motion is either stable or very weakly chaotic. In both cases, the observed stabilization should be practically constant over a rather long scale of interaction times.

The upper border of the IFS region in Fig.1 clearly follows a ω^2 law. This can be understood on the following grounds. The potential well in the ρ direction is located around $\rho \sim m\epsilon^{1/2}/\omega$ and is therefore shifted to higher and higher values of ρ as the field is increased; it will eventually move so far, that no orbit in the initial ensemble will have a chance to be trapped in it, because the initial ensemble of orbits has a finite extent in ρ , that does not depend on ϵ and ω . The critical field for this effect will clearly scale as ω^2 .

3 An aside on the autoionization of Molecules.

In our investigation of Atoms in Strong Fields we have developed a number of theoretical tools which allow for an efficient analysis of the classical dynamics of an atom in an external electromagnetic field. These methods yield a particularly efficient technique for the analysis of the stability of the motion, and for the determination of the quantitative conditions under which ionization is to be expected, due to the onset of chaos in the electron dynamics.

Although our main interest is in the Intense Field Stabilization effect, we have found that the mentioned methods are applicable to a wider class of problems. In particular, we were able to obtain significant results concerning the phenomenon of Auto-Ionization of molecular electrons - a physically important effect where classical chaos plays a determinant role.

In this Section we summarize our work on this problem, which has led us to some unexpected predictions.

3.1 Background

The study of the dynamics of electrons in molecules is conventionally based on the Born-Oppenheimer approximation, which rests on the time scale of the electronic motion being much shorter than that of the motion of the molecular core. This separation of time scales allows for a decoupling of the electronic from the core degrees of freedom. If, however, one of the electrons is excited into a Rydberg state, then its orbital frequency may

become comparable to those of the core motion, and this approximation is no more valid: the coupling between the core motion and the electron motion becomes substantial, and may also lead to ionization. This process is called auto-ionization, and is nowadays drawing attention, because recent progress in experimental technique has made it possible to prepare electrons in molecular Rydberg states.

Previous studies [13, 14, 15] have assumed that autoionization occurs only if the outer electron comes very close to the core; a condition for this should be that the angular momentum electron $l < 4$. We have instead identified a general mechanism of energy exchange between the molecular core and the Rydberg electron, which can be effective arbitrary large values of orbital momentum. This kind of interaction can lead to chaotic auto-ionization of the Rydberg electron, and can be understood by constructing a simple area-preserving map which gives the change of electron energy after one orbital period.

3.2 Theory.

Since we are interested in the case of large orbital momentum, the minimal distance $r_{\min} \approx l^2/2$ between the electron and the core is always much larger than the size of the core a . We will describe the core as consisting of a positive Coulomb charge plus a rotating dipole. For simplicity we will consider the case in which the electron orbit and the rotating dipole lie in the same plane, so that the magnetic moment $m = l$ (the case of a more general orientation of these planes qualitatively gives the same results). In this case the Hamiltonian, in atomic units, can be written in the form:

$$H = \frac{1}{2} (p_x^2 + p_y^2) + \frac{L^2}{2I} - \frac{1}{r} + d \frac{x \cos \phi + y \sin \phi}{r^3} \quad (5)$$

where d, L, I are respectively the dipole moment, the orbital momentum and the moment of inertia of the core. The angle ϕ conjugate to L gives the angle between the x -axis and the dipole direction. With the substitution $x = r \cos \varphi$, $y = r \sin \varphi$ in Hamiltonian (5), it is easily seen that $L + m = J$ is an integral of the motion; this corresponds to the conservation of the total momentum J of the molecule.

According to the Hamiltonian (5), the phase ϕ rotates with frequency $\dot{\phi} = \omega = L/I$. If the energy of rotation of the core is larger than the

change of electron energy after one orbital period, then the rotation frequency ω is approximately constant, and system (5) can be reduced to the time-dependent Hamiltonian:

$$H = \frac{1}{2} (p_x^2 + p_y^2) - \frac{1}{r} + d \frac{x \cos \omega t + y \sin \omega t}{r^3} \quad (6)$$

Moreover, since the dipole moment of the core is much less than the minimal distance r_{\min} between the electron and the core, the Hamiltonian (6) can be further approximated as:

$$H = \frac{1}{2} (p_x^2 + p_y^2) - \frac{1}{((x + d \cos \omega t)^2 + (y + d \sin \omega t)^2)^{1/2}} \quad (7)$$

If now a Kramers–Henneberger transformation [16] is performed, to a reference frame moving along a circle of radius d with angular frequency ω , then the motion becomes the same as for an Hydrogen atom in a circularly polarized monochromatic electric field, with amplitude $\epsilon = d\omega^2$. This problem was studied in detail [17, 18] where it was shown that the dynamics of the electron is described by the so called Kepler map, which gives the change of the electron energy after one orbital period:

$$\begin{aligned} \bar{N} &= N + k \sin \Phi \\ \bar{\Phi} &= \Phi + 2\pi\omega (-2\omega\bar{N})^{3/2} \end{aligned} \quad (8)$$

where $N = E/\omega$ is the electron energy $E = -1/(2n^2)$ divided by the frequency of the dipole rotation (n is the principal quantum number). The bar indicates the new values of variables after one iteration of the map. The change of electron energy given by the first equation in (8) is defined by the rotating phase $\Phi = \omega t$ of the dipole at the moment when the electron passes near the perihelion. The second equation describes the change of the rotating phase of the dipole after one orbital period. The expression for

$$k = 2.6d\omega^{1/3} \left(1 + \frac{l^2}{2n^2} + 1.09\omega^{1/3}l \right) \quad (9)$$

which gives the kick strength, was obtained in [17] and is correct in the regime where $\omega_0 = \omega n_0^3 > 1$ and when the orbital momentum $l < (3/\omega)^{1/3}$ (a

different polarization orientation gives approximately the same k -value [17]). Therefore the map (8) can be used only under the condition $d < a \ll r_{\min} \approx l^2/2 < 1/\omega^{2/3}$. A disadvantage of eq.(9) is that the kick strength k depends on l . However, according to [17], the change of l is small after one orbital period. It is also possible to show that the overall change of l during the whole ionization process is small; in fact, it is equal to the change of N (in quantum language, to the number of absorbed photons; which is quite clear, because in a circularly polarized field, the momentum of photons is equal to one, and therefore the change of the orbital momentum of the electron is equal to the number of absorbed photons). Therefore, the maximal change of l can be estimated as $\Delta l = n_0/(2\omega_0)$; in turn, if $\omega_0 > 1$, this leads to but a small change in k .

3.3 Results.

In order to check the validity of the map (8) we have numerically integrated the classical equations of motion for the original Hamiltonian (6) and we have plotted the change $\Delta N = \bar{N} - N$ over one orbital period as a function of the dipole phase at perihelion. Fig.6 shows that the numerical results agree quite well with the theoretical curve $k \sin \Phi$, with the numerical value of k in agreement with expression (9); for l we have used the initial value, because its change was relatively small. A typical structure of the phase space is shown in fig.7a which is obtained from numerical integration of Hamiltonian (6). The comparison with the phase plot (fig.7b) obtained from the Kepler map (8) further demonstrates that the map gives a good description of the dynamics.

The main conclusion which can be drawn from our analysis is that the change of the energy after one orbital period, $k\omega$, is practically independent from the minimal distance $r_{\min} \approx l^2/2$ between the electron and the core.

As it was shown in [17] the map (8) can be reduced to the celebrated standard map and, accordingly, a transition to chaotic diffusive excitation occurs when the parameter $K = 6\pi k\omega^2 n_0^5$ becomes larger than 1. This is our quantitative estimate for the onset of chaotic autoionization. Indeed, in this case the phases Φ in (8) become random and the orbit diffuses in N -space with diffusion coefficient $D = k^2/2$. This process of chaotic diffusion excitation eventually leads to ionization. The ionization time measured in the number of orbital periods is approximately $t_D = N_I^2/D$ where $N_I = 1/(2n_0^2\omega)$ is the number of photons required for ionization.

In the quantum case the situation is more complicated, and two additional borders play a relevant role. First, in order to get a significant quantum excitation, it is necessary that the so-called Shuryak stability border [20] $k = 1$ be exceeded. This essentially means that the perturbation must be larger than the unperturbed level spacing; this is a purely quantum condition, not related to the nature of the classical motion. If both conditions $K > 1, k > 1$ are fulfilled, then quantum excitation takes place. However, as it is now well-known, it may be significantly smaller than classically expected, because of quantum interference effects (localization); in that case a quantum steady state is attained, which is exponentially localized in the number of photons N around the initial state, with the localization length $\ell_\phi \approx D = k^2/2$ [17]. This implies that ionization occurs if the localization length ℓ_ϕ is larger than the number of photons N_I necessary to reach continuum. The condition $\ell_\phi = 1/(2n_0^2\omega)$ leads to the so-called quantum delocalization border $d > 1/(\omega^{5/6}n_0\sqrt{6})$.

The Shuryak condition $k > 1$ implies $d > 1/(5\omega^{5/3})$, and can be much more restrictive than the classical chaos border. For example for $n_0 = 40, \omega_0 = 4$ we have $d > 5$, much above the classical chaos border.

A qualitatively similar picture holds for the case when the dipole moment of the molecule is zero; in that case, one has to take into account a rotating *quadrupole* molecular moment.

In conclusion, the above sketched classical analysis allows for a description of the energy exchange between the rotating molecular core and Rydberg electrons. It leads to an estimate for the critical value of the interaction, above which this exchange becomes chaotic, leading to diffusive auto ionization of Rydberg electrons. Quantum effects can lead to suppression of this diffusive ionization, creating long living quasi-stationary states in the continuum spectrum of molecules. The investigation of this phenomenon in laboratory experiments will allow a better understanding of the phenomena of quantum chaos in molecular systems.

4 Conclusions and recommendations.

The analysis of the IFS model based on the model of the periodically kicked hydrogen atom has provided a fairly complete picture, which appears to be generalizable to the monochromatically driven case.. We have found that :

(1) Our estimate (3) for IFS is fully confirmed; therefore, the phenomenon takes place in a parameter range which should be accessible to present-day technology; the more so, in that

(2) this estimate is not crucially dependent on the interaction time. Concerning the dynamical origin of IFS:

(3) the stabilized motion turned out to be only weakly chaotic. Stabilization is therefore due to a significant reduction of the chaotic excitation mechanism, which, at lower field intensities, is responsible for ionization.

We have also found that the methods we have used for our theoretical analysis - a combination of the map formalism and of the Kramers-Henneberger transformation - are applicable to a wider variety of ionization problems - for example, to the chaotic autoionization of molecules.

Other important questions concerning the IFS effect were not addressed in the reported research, but appear quite accessible to our numerical and theoretical methods and, in our opinion, deserve serious attention. Among these we quote:

how robust is the IFS phenomenon against noise? A stochastic time-dependent perturbation added on the basic external driving will presumably reduce the stabilized regime. A quantitative assessment of the effect of noise would be important in the design of experiments aimed at detecting IFS.

5 Figure Captions.

1. Survival probability after a time ~ 1000 a.u., with microcanonically distributed initial conditions at $n = 1, l = 0.3, m = 0.25$, as a function of intensity ϵ and frequency ω , for 60 evenly spaced values on the horizontal axis and 80 values on the vertical axis. Darker tones of grey correspond to higher survival probability. The line has equation $\epsilon = 5.\omega/m$ and defines the Stabilization Threshold.

2. Illustrating the dependence of the ionization probability P_s on the interaction time, at fixed frequency $\omega = 7.9$, for three different field intensities: (a) $\epsilon = 0.2$; (b) $\epsilon = 3.17$; (c) $\epsilon = 500$.

3. Maximal Lyapunov Exponent λ vs. y at $x = 1$, x and y being the variables given on the horizontal and on the vertical axis, respectively, in Fig.1.

4. A typical stabilized orbit at $n = 1, m = 0.25$, initial value of $l = 0.3$, with $\epsilon = 158, \omega = 6.28$, projected onto the plane (x, y) of the initial unperturbed orbit.

5. Projection of a stabilized phase-space trajectory onto the (ρ, p_ρ) plane, for the same data as in Fig.4. Dotted lines correspond to motion in the average potential.

6. Comparison of the numerically computed values $\Delta N = \bar{N} - N$ (dots) obtained by solving the system (6) for $dn_s^{-2} = 0.000625, \omega n_s^3 = 4, l/n_s = 0.3, n_0/n_s = 1.25$ and the theoretical curve $k \sin \Phi$ (full curve), with the value of k taken from (9). The value n_s fixes the classical scale.

7. a) The phase plane (En_s^2, ϕ) for the system (6) with $dn_s^{-2} = 0.000625, \omega n_s^3 = 4, l/n_s = 0.3$. b) The phase plane obtained from the Kepler map (8) with the same parameters of case a).

6 Bibliography.

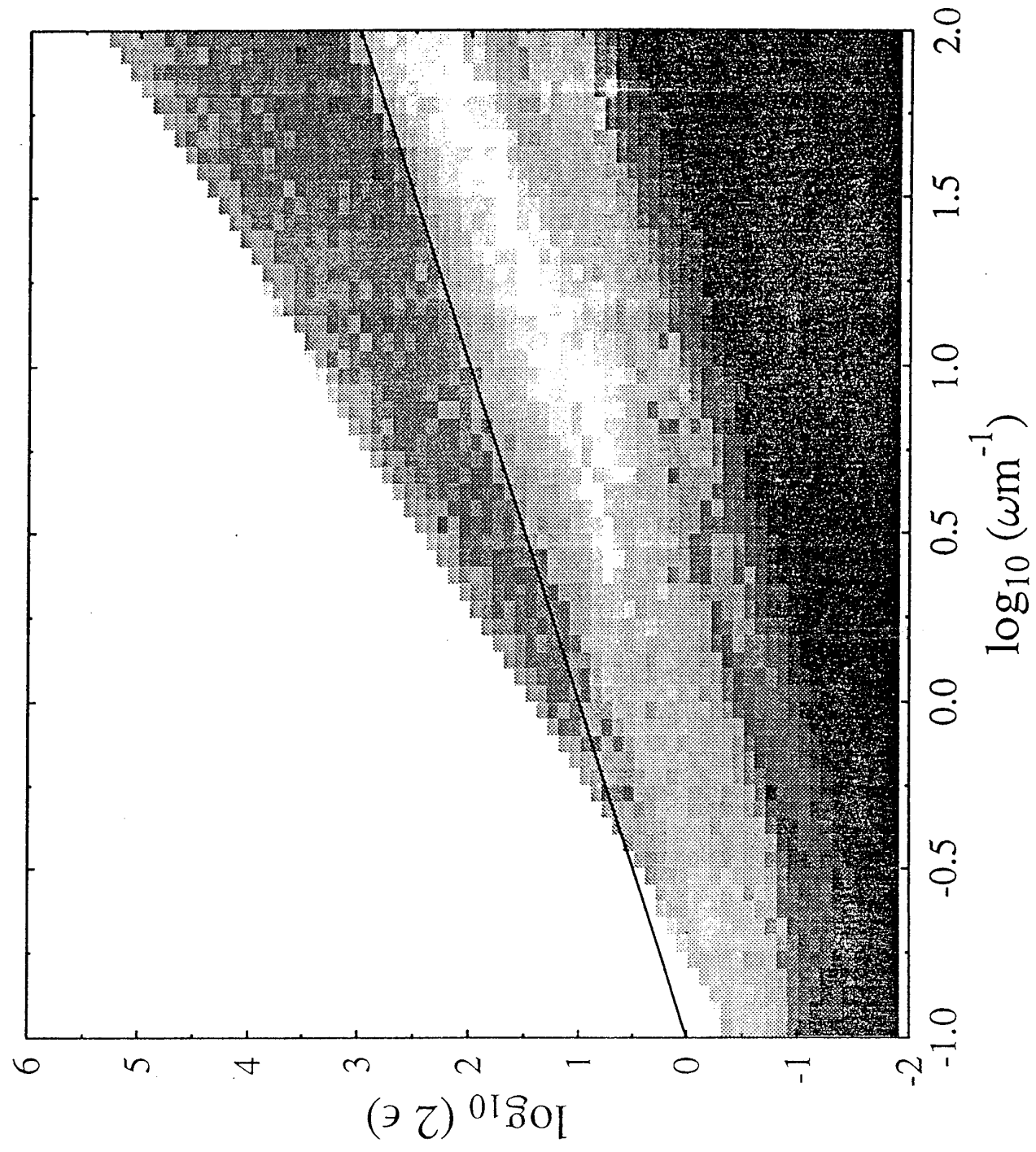
References

- [1] S.Geltman and M.R.Teague, J.Phys. B7, L22 (1974); J.I.Gersten and M.H.Mittleman, *ibidem* 9,2561 (1976); M.Gavrila and J.Z.Kaminsky, Phys. Rev.Lett. 52, 614 (1984); M.V.Fedorov and A.M.Movsesian, J.Opt.Soc.Am. B 6, 928 (1989); Q.Su, J:H:Eberly, and J.Javanainen, Phys.Rev.Lett. 64, 862 (1990); M.Pont and M.Gavrila, Phys. Rev. Lett. 65, 2362 (1990); K.C.Kulander, K.J.Schafer and J.L.Krause, *ibid.* 66, 2601 (1991); K.Burnett, P.L.Knight, B:R.M. Priraux, and V.C.Reed, *ibid.* 66, 301 (1991); V.C.Reed, P.L.Knight, and K.Burnett, *ibid.* 67, 1415 (1991);

- [2] F.Benvenuto, G.Casati and D.L.Shepelyansky, *Phys. Rev. A* **47**, R786 (1993); *Zeits. Phys. B*9 (1994).
- [3] R.V.Jensen and B.Sundaram, *Phys.Rev. A*47, 1415 (1993); *Phys.Rev. A*47, R778 (1993). **65**,1964 (1992).
- [4] Q.Su, J:H:Eberly and J.Javanainen, *Phys.Rev.Lett.* 64(1990) 862.
- [5] M.Pont and M.Gavrila, *Phys.Rev.Lett.* 65(1990) 2362
- [6] K:C:Kulander, K.J.Schafer and J.L.Krause, *Phys.Rev.Lett.* &&(1991) 2601
- [7] K.Burnett, P.L.Knight, B.R.M.Piriaux and V.C.Reed, *Phys.Rev.Lett.* 66(1991) 301
- [8] R.J.Vos and M.Gavrila, *Phys.Rev.Lett.* 68(1992) 170
- [9] C.Bowden, C.C.Sung, S.D.Pethel and A.B.Ritchie, *Phys.Rev. A*45(1992)
- [10] C.M.Bowden, S.D.Pethel, C.C.Sung and J.C.Englund, *Phys.Rev. A*46(1992)
- [11] F.Benvenuto, G.Casati and D.L.Shepelyansky, *Phys.Rev. A*45(1992)
- [12] F.Benvenuto, G.Casati and D:L:Shepelyansky, *Phys.Rev. A*47(1993) 786.
- [CGM] G.Casati, I.Guarneri and G.Mantica, *Phys. Rev. A*50 (1994) 5018.
- [13] P.Labastie, M.C.Bordas, B.Tribollet, and M.Broyer, *Phys. Rev. Lett.* **52** (1984) 1681.
- [14] J.Chevaleyre, C.Bordas, M.Broyer, and P.Labastie, *Phys. Rev. Lett.* **57** (1986) 3027.
- [15] C.Bordas, P.F.Brevet, M.Broyer, J.Chevaleyre, P.Labastie, and J.P.Perrot, *Phys. Rev. Lett.* **60** (1988) 917; M.Lombardi, P.Labastie, M.C.Bordas, and M.Broyer, *J. Chem. Phys.*, **89** (1988) 3479.
- [16] W.C.Henneberger. *Phys. Rev. Lett.* **21** (1968) 838.

- [17] G.Casati, I.Guarneri, and D.L.Shepelyansky, *IEEE J. Quantum Electron.* **QE-24** (1988) 1420.
- [18] M.Nauenberg, *Europhysics Letters*, **13** (1990) 611.
- [19] V.M.Akulin, V.Aquilanti, B.Brunetti, F.Vecchiocattivi, in "Quantum Chaos" eds. H.A.Cerdeira, R.Ramaswamy, M.C.Gutzwiller and G.Casati, World Scientific, Singapore (1991) 423; V.M.Akulin, G.Reiser and E.W.Schlag, *Chem. Phys. Lett.*, **195** (1992) 383.
- [20] E.V.Shuryak, *Zh. Eksp. Theor. Fiz.*, **71** (1976) 2039.
- [21] U.Eichmann, V.Lange and W.Sandner, *Phys. Rev. Lett.*, **68**, (1992) 21.

Fig. 1



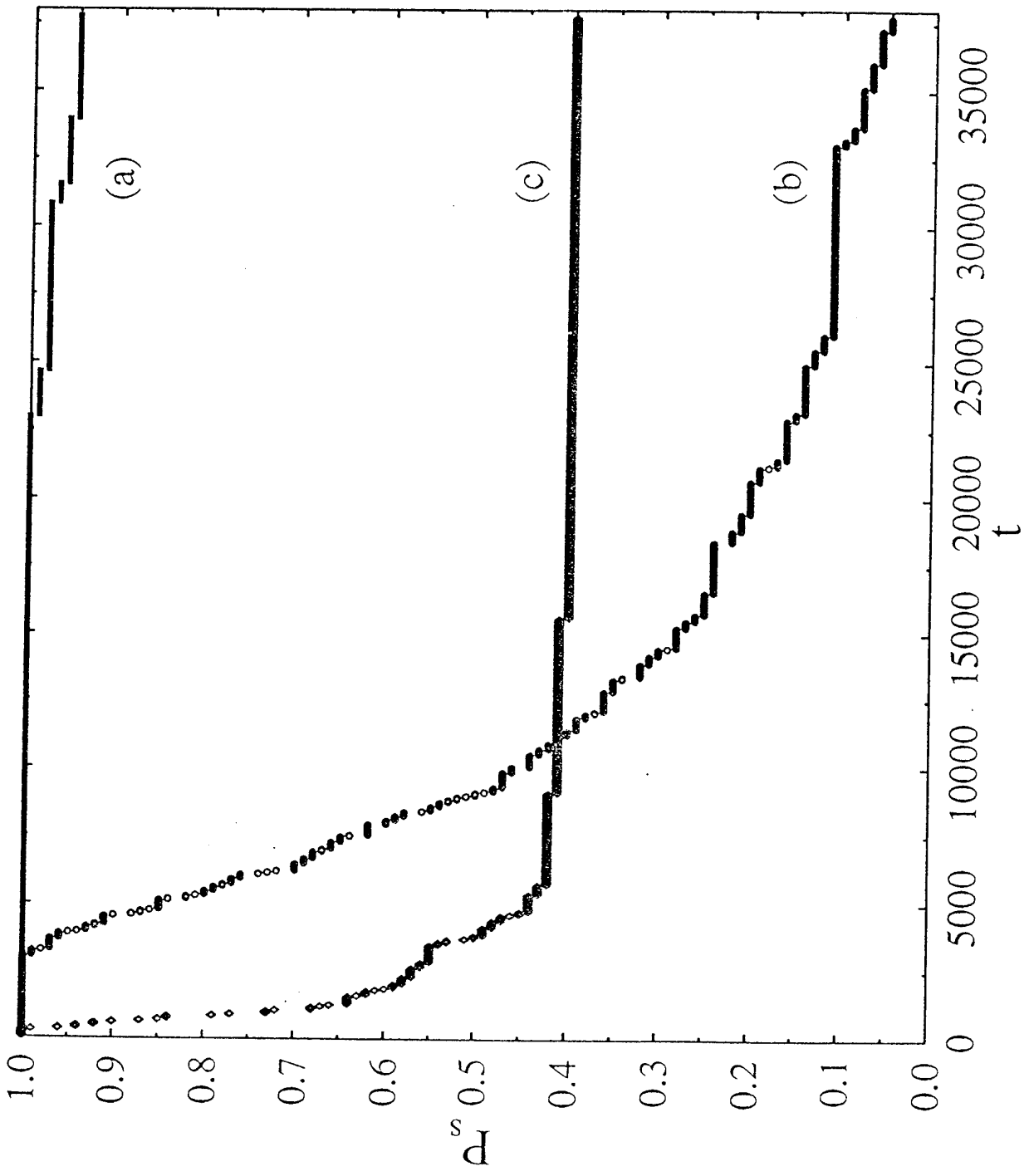


Fig. 2

Fig.3

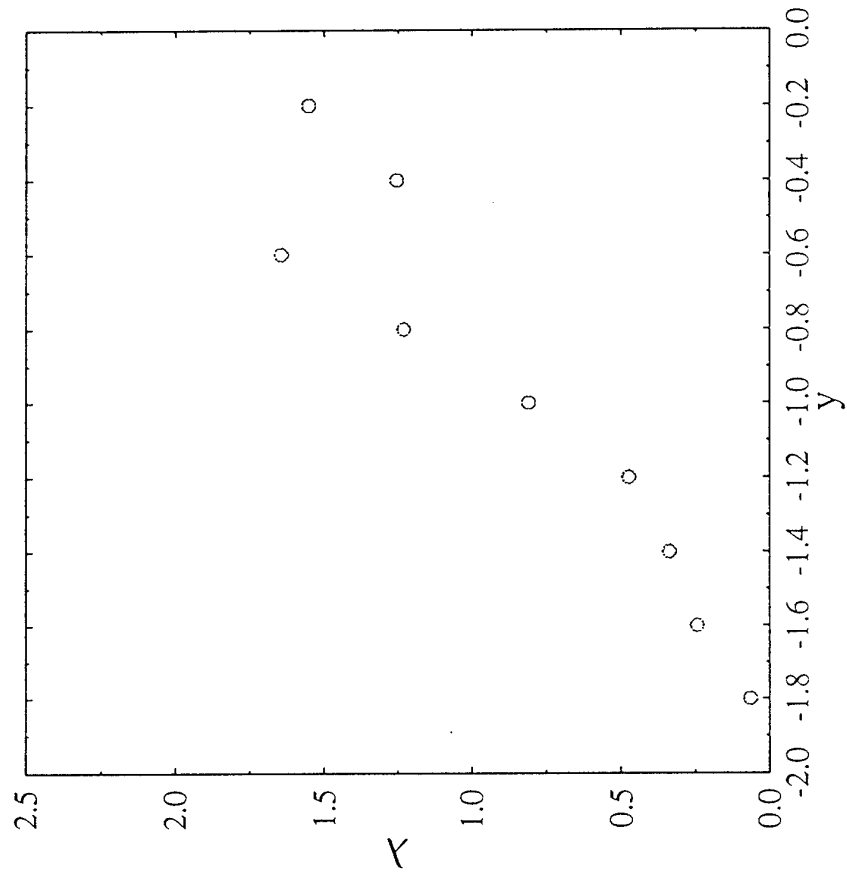


Fig. 4

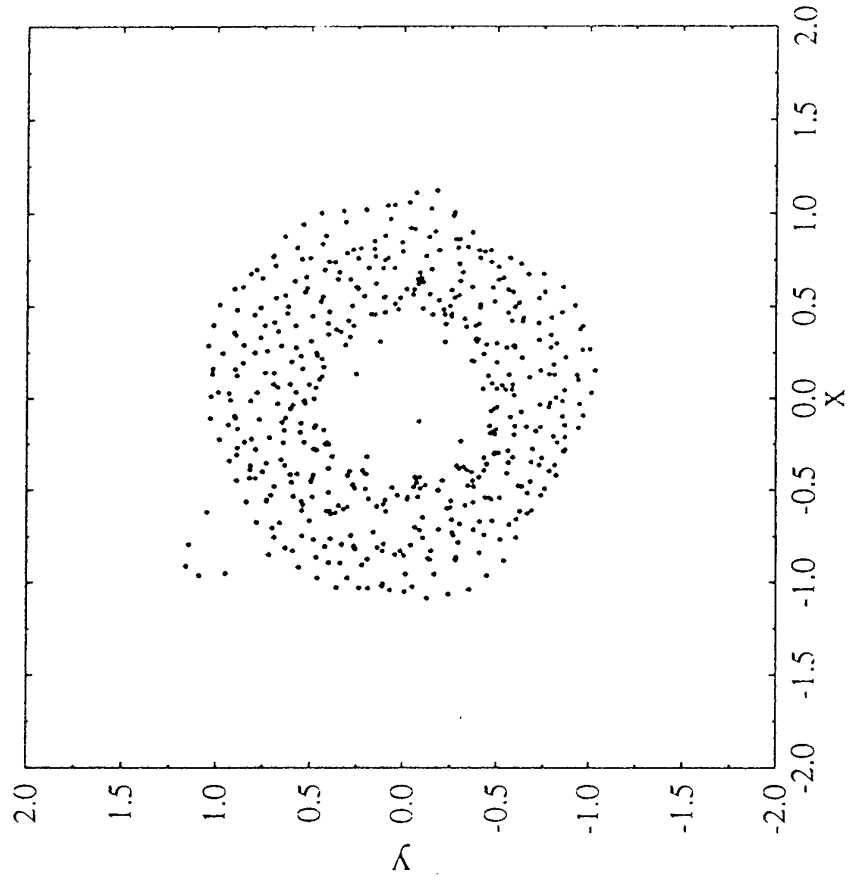


Fig.5

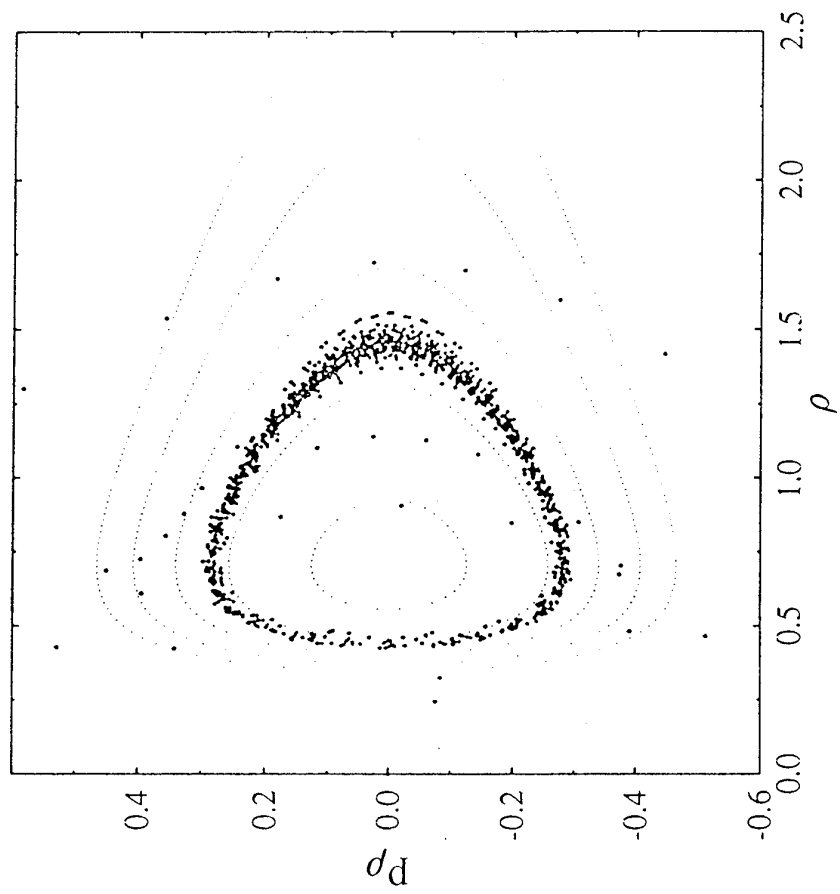


Fig. 6

$d = 0.000625$
 $\omega = 4.0$
 $n_0 = 1.25$
 $\ell = 0.3$
 $\nu = 0$

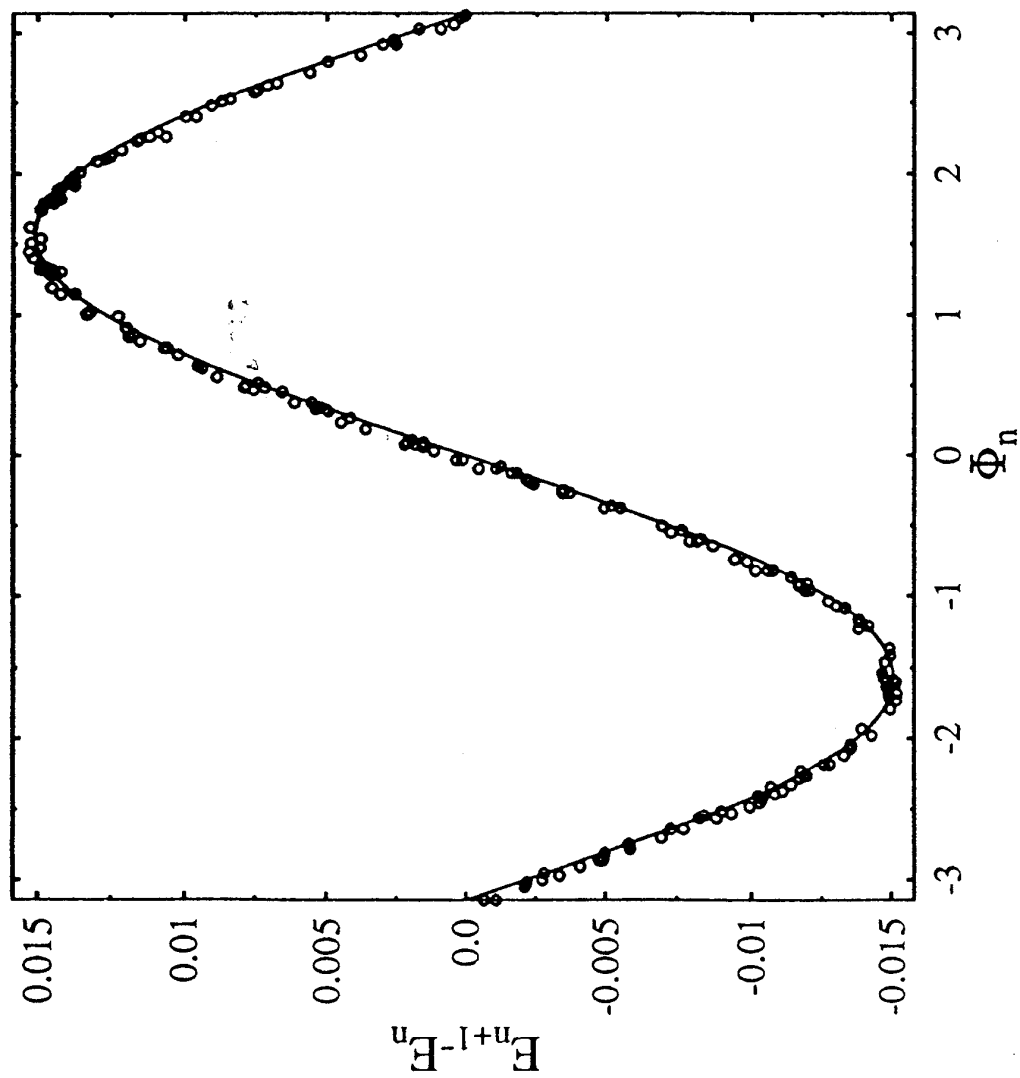


Fig. 7a
 $d = 0.000625$
 $\omega = 4.0$
 $\ell = 0.3$

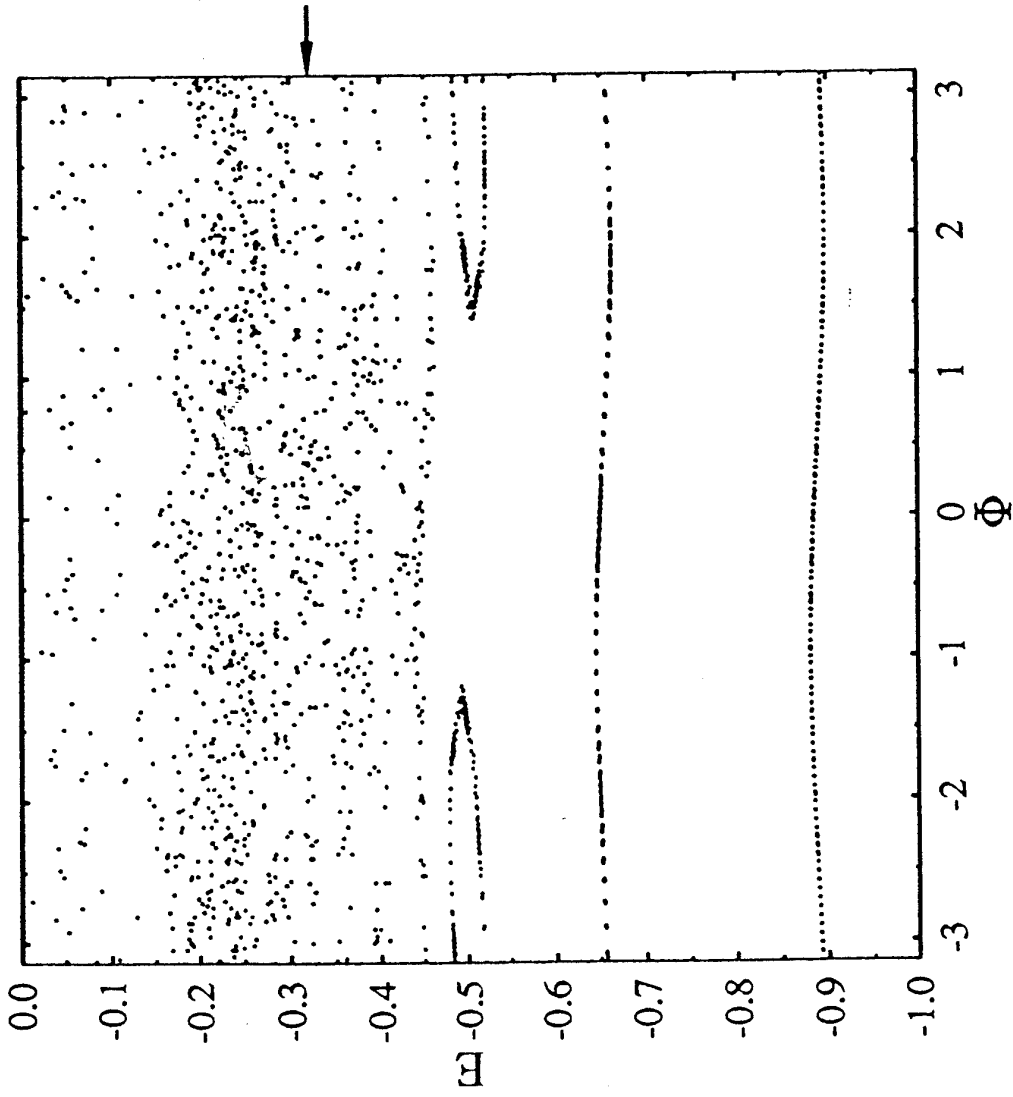


Fig. 7b (Kepler Map)

$d = 0.000625$
 $\omega = 4.0$
 $\ell = 0.3$

